Mechanisms of Ewing sarcoma metastasis : biochemistry and biophysics

Beletkaia, E.

Chapter 4

Construction of an All-Optical Controlled G-Protein Coupled Chemokine Receptor[1]

[1]Elena Beletkaia, Sylvie Olthuis-Meunier and Thomas Schmidt

G-protein coupled receptors (GPCR) occupy ∼3% of the human genome and represent a key target of the pharmaceutical market. Despite extensive development of biochemical and biophysical assays devoted to GPCR research, the development of new tools allowing achievement of a precise temporal and spatial control on the experimental system is required. Here we describe the application of the emergent high-potential research tool of optogenetics as a tool to study GPCRs. Optogenetics is based on a combination of genetic targeting and optical stimulation. We describe in detail the steps for the design and the cloning of a chimeric protein consisting of a light-activated GPCR, rhodopsin, and a chemokine receptor, CXCR4. We show that the chimeric receptor optoCXCR4 exhibits plasma membrane localization under appropriate conditions. Here we made the first steps in the development of a chimeric receptor, which could be used for further detailed investigation of CXCR4 signalling with high temporal and spatial resolution. Further developments are required to optimize optoCXCR4 application to more extended biophysical studies on GPCR signalling.

4.1 Introduction

More than 800 genes in the human genome are encoding for transmembrane G-protein coupled receptors (GPCRs) (Fredriksson et al., 2003). With this number, GPCRs represent the largest family of membrane proteins. Members of this family induce a wide variety of cellular functions, among which neurotransmission, blood pressure regulation, heart-rate regulation, and immune response, making this protein family the largest target of modern drugs. Almost half of all prescribed drugs today target GPCRs (Wess et al., 2008).

Phylogenetic analysis revealed that the GPCR family is divided into 5 sub-families as to their main physiological outcome: the adhesion family regulating tissue integrity; the secretin family controlling hormone response; the glutamate family important in neurotransmission; the frizzeled family important for embryo development; and the rhodopsin family which includes receptors for vision (Fredriksson et al., 2003). The rhodopsin family, which encompasses a wide variety of functionality, constitutes by far the largest sub-family (701 receptor) forming 4 groups: α, β, γ, δ. The δ-group of rhodopsin receptors includes the chemokine receptor cluster (Fredriksson et al., 2003). Chemokine receptors are receptors to small peptide molecules, chemokines, which are released in the body to pass information on long length scales. Activation of chemokine receptors is a key to directional cell migration called chemotaxis. Chemotaxis is essential for multiple physiological and pathological processes like embryogenesis, immune response, angiogenesis, inflammation, and metastasis.

Given their central role in inflammation and metastasis, chemokine receptors acquired quite some scientific interest. Activation of the chemokine receptors propagates biochemical reactions causing membrane protrusion formation towards higher concentrations (gradient) of the ligand. Subsequent cellular movement ultimately results in directional cell migration toward the source of ligand expression. Several models of gradient sensing were proposed. However, the direction recognition mechanism by chemokine receptors is still a topic of debate. One of the experimental challenges in the study of chemokine receptor functionality in a life cell setting is the application of precisely timed, well controlled (in terms of concentration, steepness, direction, and location) and stable chemical gradients.

Initially such chemical gradients were produced by micropipettes

filled with the chemoattractant. Although well-defined gradients could be obtained in such a way, gradients were stable only for a limited time and could be modulated only at limited frequencies. Moreover, experiments required a significant amount of material, which frequently rendered such experiments unreasonable. The development of microfluidic devices allowed the creation of long-time stable gradients which, depending on design, made high-frequency chemical modulation possible. Further, the microfluidic approach required only a minimum of material. However, compared to the earlier micropipette experiments, the microfluidics approach comprised a major disadvantage. The direction of the chemical gradient is predefined by design prior to the experiment and a gradual change in gradient direction with time is essentially impossible.

Both techniques generate gradients that extend at least on the size of a cell. Although this might reflect the situation in vivo, for some experimental designs it would be advantageous to apply a very localized chemical signal to cells, which in turn would yield a better understanding of the cytosolic signal-propagation characteristics. One approach for local cell stimulation is based on the use of chemokine-carrying beads that locally release signals when brought into contact with the cell. The position of the beads is controlled by electric or magnetic fields or by optical beams resulting in a high precision and high frequency possibility to challenge cellular response. Although this approach has been successfully applied and has become widely accessible, it adds a substantial complication to the experimental procedure.

In this current report we describe yet another approach which is based on an all-optical control of the receptor activity. We followed an optogenetic approach that has attracted much attention since the first demonstration of optical-switchable ion channels in 2003 (Nagel et al., 2003). Optogenetics is now used for targeted control of whole animals (Arenkiel et al., 2006). Through a combination of genetic targeting and optical stimulation the optogenetic approach provides a precise temporal and spatial control on the experimental system (Mattis et al., 2012). Optogenetics is currently emerging as a new, high-potential research field (Rein and Deussing, 2012; Tye and Deisseroth, 2012).

Here we developed a chimeric receptor, optoCXCR4, which was light-activated and allowed us to stimulate cellular response at high spatial and temporal resolution. Base to our chimeric receptor design is the

high structural similarity of the chemokine receptors with the comprehensively studied rhodopsin receptor. The basic concept for the design of our optoCXCR4 construct was the replacement of all intracellular parts of the rhodopsin receptor with those of the chemokine receptor CXCR4. This approach has been shown feasible earlier for the α_1- and β_2-adregeneric receptors (Airan et al., 2009). In this way receptor activation is analogous to that of rhodopsin, hence by light, whereas the intracellular signalling is controlled by the inner loops originating from the chemokine receptor of interest. The sequence design of various chimeric proteins is described in detail, followed by experiments for the characterization of their localization targeting properties and functionality. One of the chimeric receptors produced in the current study was shown to translocate successfully to the plasma membrane and display some functionality. Hence, we successfully applied an optogenetics approach to create a novel all-optical controlled chemokine receptor suitable for further biophysical studies. Whether the well-defined spatial and temporal activation of chemokine receptors in the studies of health and disease can be tackled by such optogenetic approach still has to be explored.

4.2 Materials and Methods

4.2.1 Cell culture

HEK (human embryonic kidney) 293 cells were cultivated in Dulbecco's Modified Eagle Medium (DMEM) (Sigma Life Science, USA) supplemented with 10% HyClone ™Fetal Bovine Serum (FBS, Thermo Scientific, USA), 1 mL penicillin/streptomycin (10 μg/mL antibiotics and 5 mL Glutamax™(Gibco, USA). Cells were cultured on 60 mm dishes. SH-SY5Y (human neuroblastoma) cells were cultivated in DMEM with Nutrient Mixture F-12 (DMEM/F12) supplemented with 10% FBS. Cells were cultured on T25 mattresses.

4.2.2 Sequences alignments

The protein sequence for bovine rhodopsin and CXCR4 were obtained using the Entrez databases of the National Center for Biotechnology Information (NCBI, USA). The sequence for opto-β_2AR was obtained from (Airan et al., 2009). Sequence alignments were performed using the BLAST algorithm (NCBI) or aligned manually.

4.2.3 Whole-plasmid cloning

The base-construct optoCXCR4 was modified at N- and C-terminus using a whole-plasmid cloning strategy. 20 ng of the base-construct DNA was mixed with 10 μM of forward and 10 μM of reverse primers, dNTPs, polymerase buffer, 20% DMSO and supplemented with MiliQ-water to a volume of 50 μL. Subsequently 0.25 μL of PfuX polymerase was added to run the PCR reaction. The entire plasmid was amplified in 25 cycles at a pace of 1.5 min/kB. The mixture was then incubated with 1 μL of DpnI for 1.5 hours to digest the base-construct DNA, followed by digestion with the relevant restriction enzyme (Supplemental Fig. S1 and S2) for 2 hours and ligation for 3 hours. Competent bacteria cells were transformed with the plasmid or its non-ligated analogue as control. Successful colonies were collected for amplification. DNA was purified using the DNA-purification kit following the manufacturers protocol and subsequently sequenced to check for correct sequence and/or point mutations (LGC Genomics or BaseClear).

4.2.4 Cell transfection

For experimental procedures $\sim 10^5$ cells were seeded in full medium on 35 mm dishes coated with ibiTreat (Ibidi, Germany) and incubated overnight prior to transfection. HEK 293 cells were transfected using specific ratios of FuGene HD (Promega Corporation, USA) or TurboFect (Thermo Scientific, USA) and the plasmid DNA, mixed in DMEM or OptiMEM (Life Technologies, USA). Before transfection, the medium was changed to 1 mL of corresponding serum-free medium. Then 100 μL transfection mixture was added. After the specified incubation time with the transfection mixture the medium was changed back to full medium. The cells were incubated overnight to allow for the protein expression. SH-SY5Y cells were transfected as described above, with the following modifications: the cell medium was changed to full medium approximately 6 hours before transfection, then transfection mixture was added. The cells were incubated overnight with the transfection mixtures. After incubation, the medium was changed to fresh DMEM/F12.

4.2.5 Microscopy

Imaging was performed on an Axiovert200 microscope (Zeiss, Germany) combined with a spinning disk unit (CSU-X1; Yokogawa, Japan) and

emCCD camera (iXon 897; Andor, UK). For illumination 514 (Cobolt) or 561 (Cobolt) nm lasers were used. Where indicated the CO_2 level was maintained at 5% and the temperature at 37°C using a microscopre-top unit (INUBG2E-ZILCS, TokaiHit, Japan).

4.2.6 Dual reporter activity assay

HEK 293 cells were co-transfected with the reporter element fused to the firefly luciferase (RE-*luc*), *Renilla* and one of the test sequences. We used a transfection mixture of plasmid DNA and Lipofectomine diluted separately in 12.5 μL of opti-MEM medium (Sigma Life Science, USA). Premixed components were incubated together for 20 minutes and added to the cells. After overnight incubation cells were supplemented with 100 nM of 9-cis retinal followed by 16 hours incubation. Cell activation was performed inside an incubator that was equipped with 502 nm LED illumination of uniform intensity of 200 $\mu W/cm^2$ for 6 hours. For the control (non-transfected sample) and for the sample transfected with CXCR4 (wt), activation was achieved by the addition of 100 nM of the CXCR4-specific ligand CXCL12. Subsequently the dual-luciferase detection was performed as described by the manufacturer. Briefly, cells were incubated for 15 min with luciferase assay reagent II (Promega) after which the luminescence signal was detected. Then, the cells were supplemented with Stop&Go®Reagent (Promega), which simultaneously quenches firefly luminescence and activates *Renilla* luciferase. After 15 min incubation *Renilla* luminescence was measured. The firefly luminescence was normalized to the luminescence of *Renilla*, in order to eliminate artefacts caused by, e.g. a difference in the number of cells in the sample. Further the average signals of activated samples was normalized to the average signal of non-activated samples. As negative control, samples transfected with RE-*luc* and *Renilla* only were used. All data are presented as mean of 2 to 5 independent experiments and the spread as standard deviation.

4.3 Design and characterization of an optoCXCR4 receptor

4.3.1 Design of optoCXCR4

Rhodopsin is the most extensively studied G-protein coupled receptor (GPCR). It was discovered in 1851 (Costanzi et al., 2009) and in 1970 identified as GPCR (Costanzi et al., 2009). In 1982 the receptor was sequenced (Costanzi et al., 2009) which revealed its 7-transmembrane (TM) topology. In 2000 rhodopsin was the first membrane protein for which the X-ray crystal structure was obtained (Palczewski et al., 2000).

Due to the sequence homology of the rhodopsin sub-family of GPCRs the resolved crystal structure of rhodopsin served as a base for the structure of other GPCRs of this family. The structure of a GPCR consists of three parts: (1) the extracellular, (2) the transmembrane and (3) the intracellular part (Fig. 4.1A). The extracellular part includes the N-terminus and three extracellular loops (EL1-EL3) together responsible for modulation of ligand access and ligand specificity. The transmembrane part consists of seven α-helices (TM1-TM7), forming the structural core of the receptor. The helices of the TM region are responsible for ligand recognition and signal transduction (Rajagopalan and Rajarathnam, 2006; Rosenkilde et al., 2000). The intracellular region includes intracellular loops (IL1-IL3), a small amphipathic helix (H8) and C-terminus. The intracellular parts determine downstream signalling via its G-protein binding sites on IL3 and the modulation of receptor activity on its C-terminal responsible for receptor downregulation and internalization (Venkatakrishnan et al., 2013). Thus, the TM region is thought of as communication link between the ligand-binding pocket and the G-protein-coupling region (Venkatakrishnan et al., 2013). The activation of the receptor results in its structural change. Multiple biochemical and biophysical studies suggested a common model of the TM helixes movements (Hoffmann et al., 2008; Venkatakrishnan et al., 2013; Wess et al., 2008). Mainly the TM helix 6 undergoes the largest movement (Hoffmann et al., 2008; Wess et al., 2008) inducing a rotational movement leading to a concomitant shift of the intracellular loop 3 (IL3) that controls the G-protein interaction and reorientation of its cytoplasmic end.

In contrast to all other GPCRs in which the ligand binds to the N-terminal part followed by interaction with the TM part, in rhodopsin

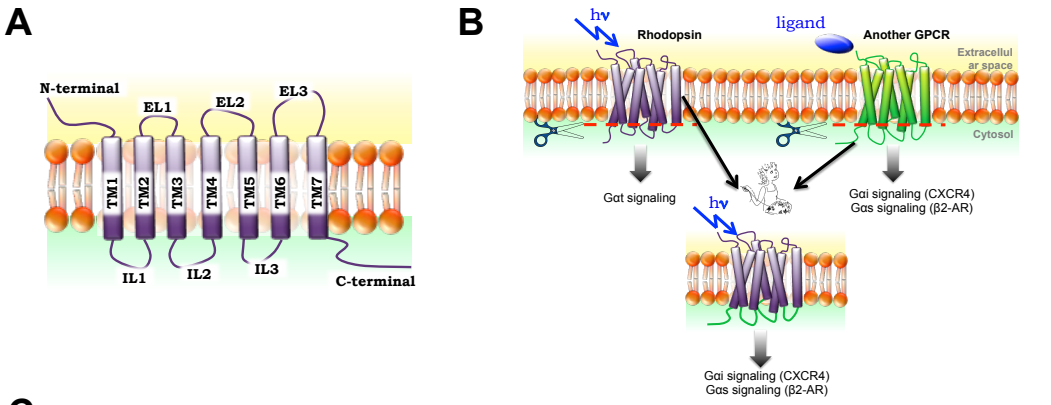

C

```
                        ————N-terminus————————————TM1————————IL1———
Bovine rhodopsin        MNGTEGPNFYVP--FSNKTGVVRSPFEAPQYYLAEPWQFS--MLAAYMFLLIMLGFPINFLTLYVTVQHKKLRTPLNYI
Human CXCR4             ---MEGISIYTSDNYTEEMGSGDYDSMKEPCFREENANFNKIFLPTIYSIIFLTGIVGNGLVILVMGYQKKLRSMTDKY
OptoCXCR4               MNGTEGPNFYVP--FSNATGVVRSPFEYPQYYLAEPWQFS--MLAAYMFLLIVLGFPINFLTLYVMGYQKKLRSMLNYI
Opto-b2AR               MNGTEGPNFYVP--FSNKTGVVRSPFEAPQYYLAEPWQFS--MLAAYMFLLIMLGFPINFLTLYVIAKFERLQTVLNYI

                        ————TM2————EL1————TM3————IL2———
Bovine rhodopsin        LLNLAVADLFMVFGGFTTTLYTSLHGYFVFGPTGCNLEGFFATLGGEIALWSLVVLAIERYVVVCKPMSNFRFGENH-
Human CXCR4             RLHLSVADLLFVIT--LPFWAVDAVANWYFGNFLCKAVHVIYTVNLYSSVLILAFISLDRYLAIVHATNSQRPRKLL-
OptoCXCR4               LLNLAVADLFMVLGGFTSTLYTSLHGYFVFGPTGCNLEGFFATLGGEIALWSLVVLAIERYVVVVHATNSQRPRKlL-
Opto-b2AR               LLNLAVADLFMVFGGFTTTLYTSLHGYFVFGPTGCNLEGFFATLGGEIALWSLVVLAIERYVVVTSPFKYQSLLTKNK

                        ————TM4————EL2————TM5————
Bovine rhodopsin        AIMGVAF-TWVMALACAAPPLVGWSRYIPEGMQCSCGIDYYTPHEETNNESFVIYMFVVHFIIPLIVIFFCYGQLVFTV
Human CXCR4             AEKVVYVGVWIPALLLTIPDFIFAN--VSEADDRYICDRFYP--NDLWVVVFQFQHIMVGLILPGIVILSCYCIIISKL
OptoCXCR4               AIMGVAF-TWVMALACAAPPLAGWSRYIPEGLQCSCGIDYYTLKPEVNNESFVIYMFVVHFTIPMIIIFFCYGIIISKL
Opto-b2AR               AIMGVAF-TWVMALACAAPPLVGWSRYIPEGMQCSCGIDYYTPHEETNNESFVIYMFVVHFIIPLIVIFFCYGR-VFQV

                        ————IL3————————————TM6———
Bovine rhodopsin        KEAAAQQQE-------------------------SATTQKAEKEVTRMVIIMVIAFLICWLPYAG------VAFYIFT
Human CXCR4             SHSKGH-QKR-----------------------------KALKTTVILILAFFACWLPYYIGISIDSFILLEII
OptoCXCR4               SHSKGH-QKR-----------------------------KALRMVIIMVIAFLICWVPYAS------VAFYIFT
Opto-b2AR               AKRQLQKIDKSEGRFHSPNLGQVEQDGRSGHGLRRSSKFCLKEHKALRMVIIMVIAFLICWLPYAG------VAFYIFT

                        ————EL3————TM7————C-terminus————
Bovine rhodopsin        HQGSDFG---PIFMTIPAFFAKTSAVYNPVIYIMMNKQFRNCMVTTLCCGKNPLGDDEASTTVSKTETSQVAPA
Human CXCR4             KQGCEFENTVHKWISITEALAFFHCCLNPILYAFLGAKFKTSAQHALTSVSRGSSLKILSKGKRGGHSSVSTESESSSFHSS
OptoCXCR4               HQGSNFG---PIFMTIPAFFAKSAAIYNPVIYIMMNKQFRTSAQHALTSVSRGSSLKILSKGKRGGHSSVSTESESSSFHSS
Opto-b2AR               HQGSDFG---PIFMTIPAFFAKTSAVYNPVIYIMMNKQFRIAFQELLCLRRSSSKAYGNGYSSNSNGKTDYMGEASGCQLGQ
                                                                EKESERLCEDPPGTESFVNCQGTVPSLSLDSQGRNCSTNDSPL
```

Figure 4.1
Design of the chimeric protein. ***A.*** *Schematic of the GPCR structure containing N-terminal, extracellular loops (EL1-EL3), transmembrane helixes (TM1-TM7), intracellular loops (IL1-IL3) and C-terminal.* ***B.*** *Schematic representation of the chimeric protein design. The IL of rhodopsin are exchanged with the IL of the GPCR of interest. The resulting chimeric receptor exhibit signalling of GPCR of interest when triggered by light activation (hν).* ***C.*** *Alignment of the bovine rhodopsin with human CXCR4 for construction of photo-activatable chimeric protein - optoCXCR4, compared to opto-β_2AR (Airan et al., 2009) .*

the ligand (retinal) is bound to the receptor though Lys_{296} (TM7) in the inactive state of the receptor. On light absorption an isomerization of retinal occurs and subsequently triggers a series of conformational changes including the rotation of TM6 leading to the G-protein activation (for review see Hofmann et al., 2009).

The high structural similarities of GPCRs including their activation scheme allowed the application of an optogenetic approach to GPCRs. It is assumed, that the precise output signal of the receptor is controlled primarily by the intracellular parts of the GPCR. Receptor activation, however, is controlled by the TM regions where the conformational change is translated into a structural change of the intracellular regions. The latter subsequently leads to the activation of G-protein dependent and independent pathways. In particular IL3 is responsible for signaling by G-proteins (either $G_{\alpha i/o}$, $G_{\alpha q/11}$, $G_{\alpha s}$ or $G_{\alpha 12/13}$ and $G_{\beta\gamma}$), while the C-terminal part of the GPCR is responsible for recognition of receptor kinases, which regulate a balanced receptor trafficking. Hence, a strategy was developed to exchange all intracellular parts and C-terminal of the rhodopsin receptor with that of another GPCR to produce a chimeric protein of particular functionality being controlled by light (Fig. 4.1B).

Kim et al. in 2005 demonstrated the feasibility of this approach with the first design of a functional all-optically activated GPCR (Kim et al., 2005). The group showed that exchange of the intracellular loops and the carboxyl (C)-terminal domain of rhodopsin with those of the β_2 adrenergic receptor ($\beta_2$2AR) results in a chimeric receptor, opto-β_2AR, which exhibited full β_2AR functionality but was light-activated. Further this chimeric-receptor approach has been demonstrated to be successful for creation of functional α_1-adregeneric receptor as well (Airan et al., 2009).

4.3.2 Cloning of various optoCXCR4 constructs

Here we designed various rhodopsin-CXCR4 chimeras following the strategy described by Kim et al. In the decision for the exact exchange positions of intracellular loops and C-terminus we were led by the alignment of the nucleotide sequence to that of rhodopsin and CXCR4, superposition of crystal structure of rhodopsin with recent crystal structure of the CXCR4 receptor (Wu et al., 2010), and by an earlier study (Xu et al., 2014). We used these findings to design an optically activated CXCR4 receptor - optoCXCR4.

A

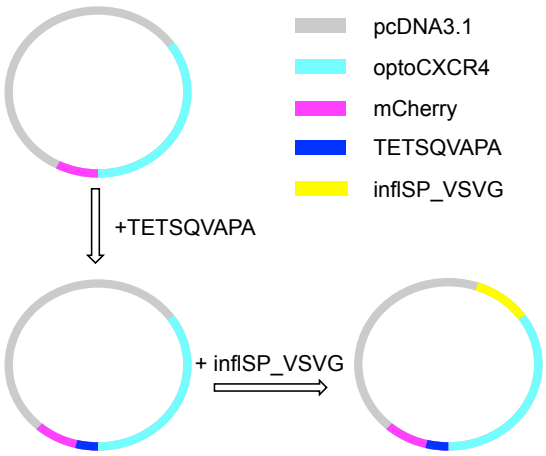

B

MHLDMNGTEGPNFYVPFSNKTGVVRSPFEAPQYYLAEPWQFSMLAAYMFLLIMLGFPINFLTLYVMGYQKKLRSMLNYILLNLAVADLFMVFGG
FTTTLYTSLHGYFVFGPTGCNLEGFFATLGGEIALWSLVVLAIERYVVVVHATNSQRPRKLLAIMGVAFTWVMALACAAPPLVGWSRYIPEGMQ
CSCGIDYYTPHEETNNESFVIYMFVVHFIIPLIVIFFCYGIIISKLSHSKGHQKRKALRMVIIMVIAFLICWLPYAGVAFYIFTHQGSDFGPIF
MTIPAFFAKTSAVYNPVIYIMMNKQFRTSAQHALTSVSRGSSLKILSKGKRGGHSSVSTESESSSFHSSTETSQVAPATGGSSGGSSGTVSKGE
EDNMAIIKEFMRFKVHMEGSVNGHEFEIEGEGEGRPYEGTQTAKLKVTKGGPLPFAWDILSPQFMYGSKAYVKHPADIPDYLKLSFPEGFKWER
VMNFEDGGVVTVTQDSSLQDGEFIYKVKLRGTNFPSDGPVMQKKTMGWEASSERMYPEDGALKGEIKQRLKLKDGGHYDAEVKTTYKAKKPVQL
PGAYNVNIKLDITSHNEDYTIVEQYERAEGRHSTGGMDELYK*

C

MKTIIALSYIFCLVFAMYTDIEMNRLGKDSLMNGTEGPNFYVPFSNKTGVVRSPFEAPQYYLAEPWQFSMLAAYMFLLIMLGFPINFLTLYVMG
YQKKLRSMLNYILLNLAVADLFMVFGGFTTTLYTSLHGYFVFGPTGCNLEGFFATLGGEIALWSLVVLAIERYVVVVHATNSQRPRKLLAIMGV
AFTWVMALACAAPPLVGWSRYIPEGMQCSCGIDYYTPHEETNNESFVIYMFVVHFIIPLIVIFFCYGIIISKLSHSKGHQKRKALRMVIIMVIA
FLICWLPYAGVAFYIFTHQGSDFGPIFMTIPAFFAKTSAVYNPVIYIMMNKQFRTSAQHALTSVSRGSSLKILSKGKRGGHSSVSTESESSSFH
SSRTQPVEICCTVSKGEEDNMAIIKEFMRFKVHMEGSVNGHEFEIEGEGEGRPYEGTQTAKLKVTKGGPLPFAWDILSPQFMYGSKAYVKHPAD
IPDYLKLSFPEGFKWERVMNFEDGGVVTVTQDSSLQDGEFIYKVKLRGTNFPSDGPVMQKKTMGWEASSERMYPEDGALKGEIKQRLKLKDGGH
YDAEVKTTYKAKKPVQLPGAYNVNIKLDITSHNEDYTIVEQYERAEGRHSTGGMDELYK*

MKTIIALSYIFCLVFAMYTDIEMNRLGKDSLMNGTEGPNFYVPFSNKTGVVRSPFEAPQYYLAEPWQFSMLAAYMFLLIMLGFPINFLTLYVMG
YQKKLRSMLNYILLNLAVADLFMVFGGFTTTLYTSLHGYFVFGPTGCNLEGFFATLGGEIALWSLVVLAIERYVVVVHATNSQRPRKLLAIMGV
AFTWVMALACAAPPLVGWSRYIPEGMQCSCGIDYYTPHEETNNESFVIYMFVVHFIIPLIVIFFCYGIIISKLSHSKGHQKRKALRMVIIMVIA
FLICWLPYAGVAFYIFTHQGSDFGPIFMTIPAFFAKTSAVYNPVIYIMMNKQFRTSAQHALTSVSRGSSLKILSKGKRGGHSSVSTESESSSIH
SSTETSQVAPATGGSSGGSSGTVSKGEEDNMAIIKEFMRFKVHMEGSVNGHEFEIEGEGEGRPYEGTQTAKLKVTKGGPLPFAWDILSPQFMYG
SKAYVKHPADIPDYLKLSFPEGFKWERVMNFEDGGVVTVTQDSSLQDGEFIYKVKLRGTNFPSDGPVMQKKTMGWEASSERMYPEDGALKGEIK
QRLKLKDGGHYDAEVKTTYKAKKPVQLPGAYNVNIKLDITSHNEDYTIVEQYERAEGRHSTGGMDELYK*

Figure 4.2
Design of enhanced optoCXCR4 plasmids. ***A.*** *Schematic representation of the addition of the C-terminus amino acids of rhodopsin -TETSQVAPA (dark blue), and the influenza SP - VSV g-epitope (yellow) to optoCXCR4-mCherry (light blue - pink).* ***B.*** *Amino-acid sequence of the final optoCXCR4-TETSQVAPA-mCherry plasmid.* ***C.*** *Amino-acid sequence of the final inflSP_VSVG-optoCXCR4-mCherry (top) and inflSP_VSVG-optoCXCR4-TETSQVAPA-mCherry (bottom) plasmids.*

In our base-design the intracellular loops and the C-terminus of the chimeric receptor were identical to those of human CXCR4, the rest was equal to that of rhodopsin (Fig. 4.2B,C). The rhodopsin intracellular loop IL1 (V_{61}-I_{75}) was replaced starting from T_{62} with IL1 of CXCR4 (M_{63}-M_{72}). Similarly, IL2 of rhodopsin (Y_{135}-H_{151}) was replaced starting from C_{139} with IL2 of CXCR4 (V_{139}-L_{151}). Rhodopsin-IL3 (Q_{224}-R_{251}) was completely replaced with IL3 of CXCR4 (I_{221}-L_{239}). Finally, the C-terminal part of rhodopsin was exchanged five amino acids after TM7 (N_{309}-R_{314}) with the C-terminal part of CXCR4 (T_{311}-S_{352}). Furthermore, at the C-terminus the construct was fused to either of the fluorescent proteins YFP or mCherry to enable visualization of the chimeric receptor. This base-design for an optoCXCR4 containing 355 amino acids was translated into a DNA sequence optimized for mammalian expression, synthesized (Genscript) and cloned into the pUC57 plasmid vector (Invitrogen). For further application we subsequently re-cloned the construct into the pcDNA3.1(+)-eYFP C1 vector.

Additionally to the base-construct we designed other constructs with modifications to the N- and C-terminus in order to putatively facilitate protein trafficking and assist proper protein targeting (Fig. 4.2).

To facilitate protein trafficking the last 9 amino-acids of the C-terminal domain of rhodopsin (TETSQVAPA) were added to the C-terminal of the base-construct. The QVS(A)PA amino-acid sequence is highly conserved for various opsins and shown to play an essential role in the formation of post-Golgi vesicles (Deretic, 1998; Deretic et al., 1998). Mutations in the C-terminal region of rhodopsin caused mislocalization of the protein (Deretic, 1998). To introduce the C-terminal sequence of rhodopsin (TETSQVAPA) a cloning technique based on PCR multiplication of the entire plasmid was used. We designed primers with homologous sequences to optoCXCR4-mCherry and the TETSQVAPA sequence as shown in the Supplementary Fig. S1. The whole-plasmid cloning procedure was performed as detailed in the Materials and Methods section. The final amino-acid sequence of optoCXCR4-TETSQVAPA-mCherry (further referred to as optoCXCR4-C9) is shown in Fig. 4.2B.

Further, we added a signalling peptide to the N-terminus of the base-construct to assist proper protein targeting towards the plasma membrane. It has been demonstrated that a N-terminal signalling peptide is required for receptor translocation across the endoplasmic reticulum (ER). GPCRs lacking this signalling peptide were retained in the ER

in a non-functional form (Kochl et al., 2002). As a N-terminal signalling motif we used an epitope of the vesicular stomatitis virus-G protein (VSVG) followed by the influenza A signalling peptide (inflSP). VSVG is a trans-membrane glycoprotein that contains a six amino acid signalling sequence facilitating efficient export of the protein from the endoplasmatic reticulum (ER). VSVG enhances viral envelope fusion with the plasma membrane (Roche et al., 2008). The six-residue epitope was shown to be sufficient for enhanced ER export (Sevier et al., 2000). For cloning the whole-plasmid strategy was used. Given that the inflSP-VSVG sequence was too long to be coded into one primer, a silent mutation was introduced in the middle of the sequence to create a restriction site (Supplementary Fig. S2). That allowed us to incorporate inflSP-VSVG in such a way, that one part was included in forward and the other in reverse primer. Using optoCXCR4-mCherry and optoCXCR4-TETSQVAPA-mCherry as base-construct DNA, we generated inflSP_VSVG-optoCXCR4-TETSQVAPA-mCherry and inflSP_VSVG-optoCXCR4-mCherry plasmids (further referred to as v-optoCXCR4-C9 and v-optoCXCR4, respectively) encoding the desired inflSP_VSVG sequence with or without the TETSQVAPA sequence (Fig. 4.2C).

In total five plasmids were created including the base-construct optoCXCR4: optoCXCR4-YFP, optoCXCR4-mCherry, optoCXCR4-C9, v-optoCXCR4 and, v-optoCXCR4-C9.

4.3.3 Optimization of cell transfection

Human embryonic kidney HEK 293 cells have a substantial endogenous expression of CXCR4. Thus, this cell line appeared as an appropriate system to follow optoCXCR4 signalling. We first optimized the transfection conditions for HEK 293 cells with the optoCXCR4 constructs using two different transfection reagents: FuGene and TurboFect. For transfections with FuGene 6 to 20 μL of reagent was mixed with 0.5-2 μg of plasmid DNA resulting in reagent:DNA ratios of 3:1, 6:1, 10:1 and 12:1. The incubation time with the FuGene-based transfection mixtures was kept at 3 hours. For transfections with TurboFect, 1-4 μL of the reagent were mixed with 1 μg of plasmid DNA resulting in reagent:DNA ratios of 1:1, 2:1 and 4:1. T he incubation time for TuboFect-based transfection mixtures ranged from 0.5-2 hours. We found that using 4 μL of TurboFect, 1 μg of DNA and 1.5 hours of incubation time led to optimal

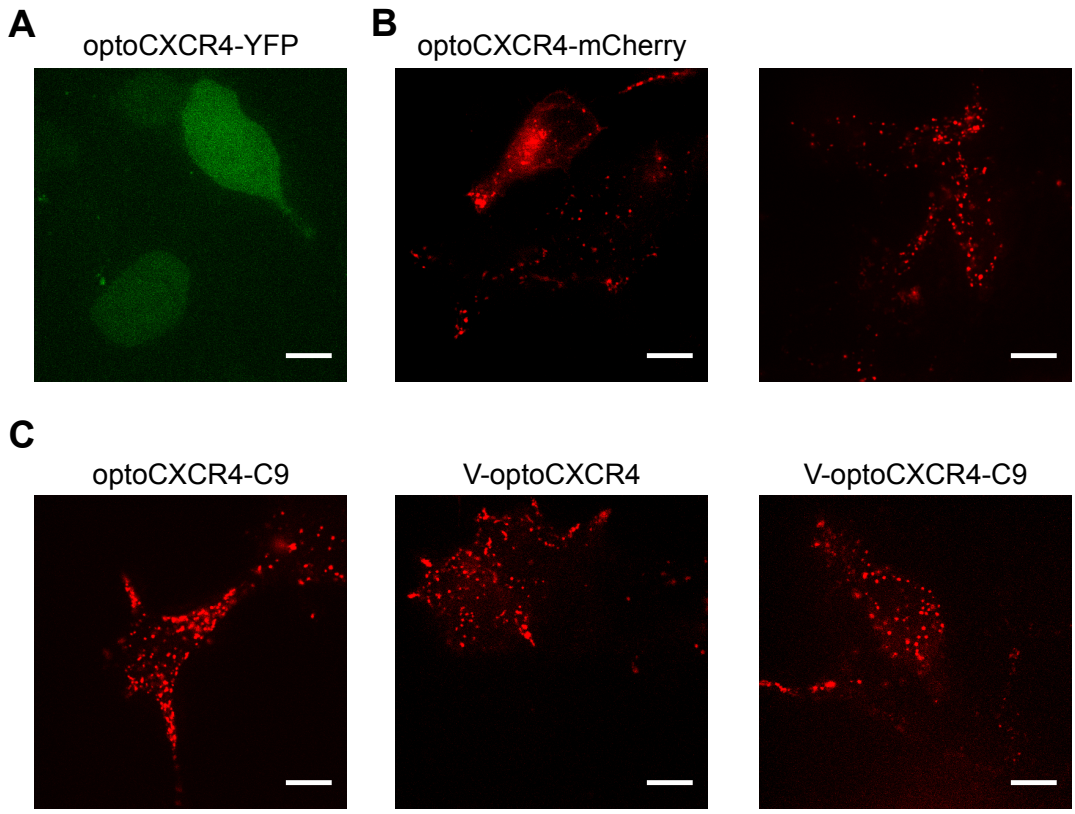

Figure 4.3
Transfection with optoCXCR4. ***A.*** *HEK 293 cells transfected with optoCXCR4-YFP using 1.5 hours of incubation with a transfection mixture containing 4 µL of TurboFect and 1 µg of DNA.* ***B.*** *HEK 293 cells transfected with optoCXCR4-mCherry using same transfection protocol after 1 (left) or 3 (right) days of expression.* ***C.*** *HEK 293 cells transfected with different variants of optoCXCR4-mCherry plasmid. Scale bar - 10 µm.*

transfection condition. the transfection efficiency was estimated from the percentage of fluorescent cells, 30-50% (data not shown). Hence, this transfection protocol was used for all further experiments on HEK 293 cells with optoCXCR4, if not indicated otherwise.

4.3.4 Localization of the chimeric receptors

To check the localization of the chimeric protein we performed fluorescence imaging on transfected HEK 293 cells. Imaging was done using spinning-disk confocal microscopy with 514 nm and 561 nm laser excitation for YFP- and mCherry-fused constructs, respectively. As shown in Figure 4.3 the chimeric proteins did not exhibit any pronounced

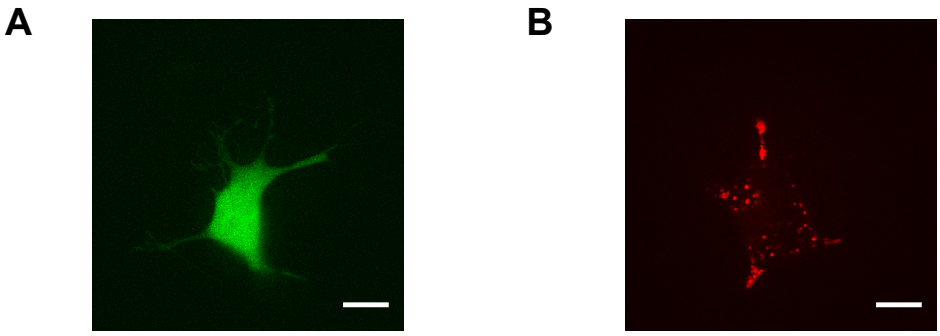

Figure 4.4
Localization of retinal-supplemented optoCXCR4-YFP. ***A.*** *SH-YSY5 cells transfected with optoCXCR4.* ***B.*** *HEK 293 cells transfected with optoCXCR4-mCherry plasmid after overnight incubation with 100 nM 9-cis retinal. Scale bar - 10 μm.*

plasma membrane localization. The fluorescent signals indicated that the optoCXCR4-YFP protein was uniformly distributed throughout the cell (Fig. 4.3A) and the optoCXCR4-mCherry protein presumably localized in vesicular structures (Fig. 4.3B, left). A longer incubation time after transfection did not change the localization of the optoCXCR4 constructs (Fig. 4.3B, right). Surprisingly, vesicular localization was observed for optoCXCR4-C9, v-optoCXCR4 and v-optoCXCR4-C9 constructs that were expected to exhibit enhanced plasma membrane targeting (Fig. 4.3C).

To avoid receptor activation during imaging the experiments described in Figure 4.3 were performed without addition of retinal, the rhodopsin ligand. Since it is unclear whether HEK 293 cells produced retinal endogenously, we questioned whether lack of the ligand might cause a disruption in the protein folding or protein targeting. Hence, we repeated the experiments in the neuroblastoma-derived cell line, SH-YSY5, which was shown to express both receptors CXCR4 and rhodopsin endogenously (Liberman et al., 2012; Saliba et al., 2002), and supposedly also produced the retinal. SH-YSY5 cells were transfected as described in Materials and Methods section. Confocal imaging of transfected SH-YSY5 cells was performed after overnight incubation. However, similar to our findings in HEK 293, optoCXCR4-YFP did not show any pronounced plasma membrane localization (Fig. 4.4A). Likewise, overnight incubation of HEK 293 cells with 100 nM of 9-cis retinal did not alter the localization of the chimeric receptor (Fig. 4.4B). Hence, the mislo-

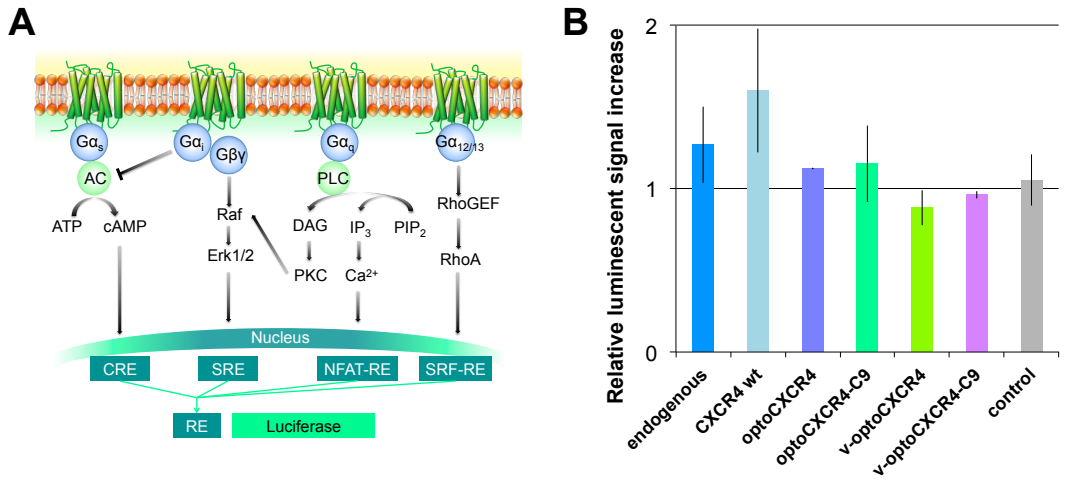

Figure 4.5
Luciferase assay. ***A.*** *Schematic representation of the luciferase assay adopted from Promega (Literature # TM040).* ***B.*** *Relative increase of the luciferase luminescence detected in HEK 293 cells for different constructs.*

calization of optoCXCR4 could not be attributed to the absence of the ligand.

Another potential reason for the mislocalization of the optoCXCX4 constructs could be due to receptor activation and initiation of the G-protein signalling cascade followed by a fast internalization of the receptor. Hence, the vesicular localization could potentially be attributed to the functionality of the receptor.

4.3.5 Functionality of the optoCXCR4 constructs

We tested the various optoCXCR4 constructs for functionality by analysing the G-protein activity using a dual-reporter luciferase assay (for details see Materials and Methods). HEK 293 cells were co-transfected with one of the optoCXCR4 constructs together with a reporter luciferase (Re-*luc*) and a *Renilla* luciferase construct. The Re-*luc* construct contains the firefly luciferase gene placed downstream of G-protein specific response elements (REs) (Fig. 4.5A). Stimulation of the receptor results in activation of a specific G-protein. In turn, the downstream biochemical cascade triggers the respective transcription factors that bind to the REs leading to luciferase expression. Luminescence of the *Renilla* luciferase was used to normalize the Re-*luc* luminescence for each sample.

For our experiments the $G_{\alpha i}/G_{\alpha 12}$-RE was used. Figure 4.5B shows the increase of relative luciferase luminescence for the various optoCXCR4 constructs after light stimulation. Cells transfected with the CXCR4 (wt) construct stimulated by 100 nM CXCL12 were used as a positive control. All data are presented as the relative change in the luciferase luminescence after stimulation with respect to the luciferase luminescence for non-stimulated cells. As negative control, light-activated cells transfected with Re-*luc* and *Renilla* but without any optoCXCR4 construct were used.

As expected, cells that contain either endogenous CXCR4 or that were transfected with a CXCR4 (wt) construct exhibited a relative luciferase luminescence increase of 1.2±0.2 and 1.6±0.4 after stimulation with CXCL12, respectively. Light activation of the optoCXCR4 and optoCXCR4-C9 constructs resulted in a relative luciferase increase of 1.1±0.1 and 1.2±0.2, respectively. The v-optoCXCR4 and v-optoCXCR4-C9 constructs exhibited a relative luminescence change of 0.9±0.1 and 1.0±0.1, respectively. Hence, within error-bars the activity of all optoCXCR4 constructs were not different to that of the negative control cells (1.1±0.2).

The negative results should not be taken as conclusive. In preparation of the dual-reporter assay cells were frequently exposed to light, which presumably leads to fast internalization of the chimeric receptors, and concomitantly to the inability to activate the G-protein pathways.

4.3.6 Fast optoCXCR4 internalization

Many GPCRs are known to undergo internalization upon continued activation. The internalization process in GPCRs is related to cellular adaptation, which allows cells to properly function in a wide concentration range of the ligand. We (Chapter 2 of this thesis), and others (Venkatesan, 2003) have reported that CXCR4 is efficiently internalized after stimulation with its natural ligand CXCL12.

Stimulation of rhodopsin by light is an extremely efficient process. The absorption of a single photon in the range between 400 and 600 nm suffices for receptor activation. In the experiments described above, we assumed that optoCXCR4 was inactive when it was not loaded with 9-cis retinal. However, any presence of retinal in the culture medium or plausible endogenous production of retinal in HEK 293 cells could not be completely excluded. Hence, we performed an experiment in complete dark-

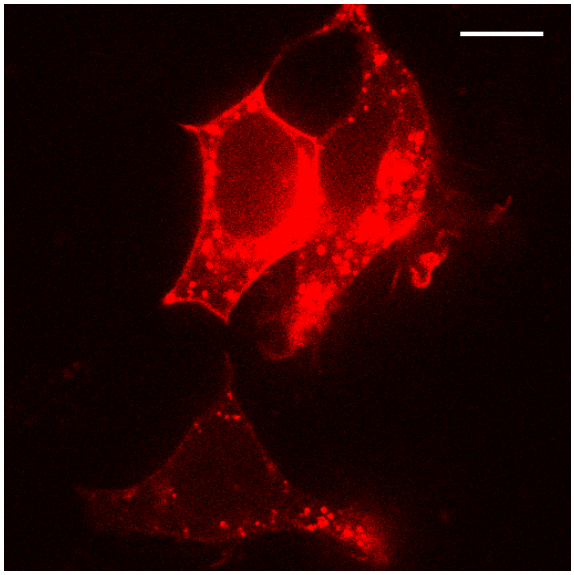

Figure 4.6
Transfection with optoCXCR4-mCherry. HEK 293 cells imaged 12 hours after transfection with optoCXCR4-mCherry plasmid. Extra precaution was taken to keep the cells in dark during the whole experimental procedure. Scale bar - 10 μm.

ness and limited the subsequent imaging time to 20 minutes. HEK 293 cells where transfected and incubated in a light-protected microscope-top incubator at 5% CO2 and 37°C (INCUBG2E-ZILS, Tokai Hit). After 12 hours the cells were imaged without additional steps. Following this transfection procedure resulted in localization of the optoCXCR4-mCherry largely at the plasma membrane (Fig. 4.6). This result implies that the cytosolic localization of the optoCXCR4 constructs in the earlier experiments was related to receptor internalization. Hence, the continued receptor stimulation during experiment preparation led to the receptor internalization and loss of the plasma membrane localization.

4.4 Conclusions

Here we described the construction of an all-optical controllable chemokine G-protein coupled receptor optoCXCR4. Inasmuch as the activation of rhodopsin is extremely fast and efficient, the optoCXCR4 protein was destined for internalization shortly after activation. A functional and correctly localized chimeric receptor was only observed when all preparatory steps were performed in complete darkness. A successful application of

optogenetic approach to GPCRs in cell-based or whole animal experiments have been shown by various groups. Nevertheless, it appears that further development is required to optimize this promising research tool for biophysical studies on GPCR dynamics at high special and temporal control. One way might be to make a design based on color opsins, which have a narrower excitation band, making imaging without receptor activation more feasible. Another way might include the use of bistable pigments. The bistable pigments can convert isomerized retinal into the pre-activated state: they contain an intrinsic bleach-recovery system and, thus, are capable of repeated activation of the receptor. (Bailes et al., 2012; Tsukamoto and Terakita, 2010)

4.5 Supplemental figures

Forward primer:

- Start point +AgeI +linker(GSSGGSSG) +homologus part
  - gatcaccggtggaagctctggcggatccagtggtacagtgagcaagggcgagg

Reverse primer:

- Start point + AgeI +TETSQAPA +homologus part (reverse)
  - gatcaccggtggcaggcgccacttggctggtttctgtgctgctatgaaagctgctgc

atgaacggcaccgaaggcccgaacttttatgtgccgtttagcaacaaaaccggcgtggtgcgcagcccgtttgaagcgccgcagtattatctgg
cggaaccgtggcagtttagcatgctggcggcgtatatgtttctgctgattatgctgggctttccgattaactttctgaccctgtatgtgatggg
ctatcagaaaaaactgcgcagcatgctgaactatattctgctgaacctggcggtggcggatctgtttatggtgtttggcggctttaccaccacc
ctgtataccagcctgcatggctattttgtgtttggcccgaccggctgcaacctggaaggctttttgcgacccctgggcggcgaaattgcgctgt
ggagcctggtggtgctggcgattgaacgctatgtggtggtggtgcatgcgaccaacagccagcgcccgcgcaaactgctggcgattatgggcgt
ggcgtttacctgggtgatggcgctggcgtgcgcggcgccgccgctggtgggctggagccgctatattccggaaggcatgcagtgcagctgcggc
attgattattataccccgcatgaagaaaccaacaacgaaagctttgtgatttatatgtttgtggtgcattttattattccgctgattgtgattt
ttttttgctatggcattattattagcaaactgagccatagcaaaggccatcagaaacgcaaagcgctgcgcatggtgattattatggtgattgc
gtttctgatttgctggctgccgtatgcgggcgtggcgttttatatttttacccatcagggcagcgattttggcccgatttttatgaccattccg
gcgttttttgcgaaaaccagcgcggtgtataacccggtgatttatattatgatgaacaaacagtttcgcaccagcgcgcagcatgcgctgacca
gcgtgagccgcggcagcagcctgaaaattctgagcaaaggcaaacgcggcggccatagcagcgtgagcaccgaaagcgaaagcagcagctttca
tagcagccgtacgcaaccggtcgagatctgctgtacagtgagcaagggcgaggaggataacatggccatcatcaaggagttcatgcgcttcaag
gtgcacatggagggctccgtgaacggccacgagttcgagatcgagggcgagggcgagggccgcccctacgagggcacccagaccgccaagctga
aggtgaccaagggtggccccctgcccttcgcctgggacatcctgtcccctcagttcatgtacggctccaaggcctacgtgaagcaccccgccga
catccccgactacttgaagctgtccttccccgagggcttcaagtgggagcgcgtgatgaacttcgaggacggcggcgtggtgaccgtgacccag
gactcctccctccaggacggcgagttcatctacaaggtgaagctgcgcggcaccaacttcccctccgacggccccgtaatgcagaagaagacca
tgggctgggaggcctcctccgagcggatgtaccccgaggacggcgccctgaagggcgagatcaagcagaggctgaagctgaaggacggcggcca
ctacgacgctgaggtcaagaccacctacaaggccaagaagcccgtgcagctgccccggcgcctacaacgtcaacatcaagttggacatcacctcc
cacaacgaggactacaccatcgtggaacagtacgaacgcgccgagggccgccactccaccggcggcatggacgagctgtacaagtag

Figure S1
Design of primers for TETSQVAPA cloning. The forward primer contains a starting sequence, specific restriction enzyme AgeI (green), linker sequence and sequence homologues to the base-construct DNA. The reverse primer contains a starting sequence, specific restriction enzyme AgeI (green), TETSQAPA sequence and sequence homologues to the base-construct DNA. Start codon and spot codon are colored red, the sequence of CXCR4 highlighted in blue, the sequence of mCherry - in pink.

inflSP_VSV-Gepitope
accatgaagacgatcatcgccctgagctacatcttctgcctggtattcgccatgtacaccGATATAgagatgaacaggctgggaaaggatagcc
tc

point mutation to create silent EcoRV site
accatgaaaacgatcatcgccctgagctacatcttctgcctggtattcgccatgtacaccGATATCgagatgaacaggctgggaaaggatagcc
tc

Forward primer:

- Start point +EcoRV and part of inflSP_VSV-g-epitope +homologos part
  - gatcGATATCgagatgaacaggctgggaaaggatagcctcatgaacggcaccgaaggc

Reverse primer:

- start point +EcoRV and part of inflSP_VSV-g-epitope +homologus part (reverse)
  - gatcGATATCggtgtacatggcgaataccaggcagaagatgtagctcagggcgatgatcgttttcatggtaccaagcttaagtttaaa

cgaaattaatacgactcactatagggagacccaagctggctagcgtttaaacttaagcttggtacctcgcgaatgcatctagatatgaacggca
ccgaaggccgaactttatgtgccgtttagcaacaaaaccggcgtggtgcgcagcccgtttgaagcgccgcagtattatctggcggaaccgtg
gcagtttagcatgctggcggcgtatatgtttctgctgattatgctgggctttccgattaactttctgaccctgtatgtgatgggctatcagaaa
aaactgcgcagcatgctgaactatattctgctgaacctggcggtggcggatctgtttatggtgtttggcggctttaccaccaccctgtatacca
gcctgcatggctattttgtgtttggcccgaccggctgcaacctggaaggctttttgcgaccctgggcggcgaaattgcgctgtggagcctggt
ggtgctggcgattgaacgctatgtggtggtggtgcatgcgaccaacagccagcgcccgcgcaaactgctggcgattatgggcgtggcgtttacc
tgggtgatggcgctggcgtgcgcggcgccgccgctggtgggctggagccgctatattccggaaggcatgcagtgcagctgcggcattgattatt
ataccccgcatgaagaaaccaacaacgaaagctttgtgatttatatgtttgtggtgcattttattattccgctgattgtgatttttttttgcta
tggcattattattagcaaactgagccatagcaaaggccatcagaaacgcaaagcgctgcgcatggtgattattatggtgattgcgtttctgatt
tgctggctgccgtatgcgggcgtggcgttttatatttttacccatcagggcagcgattttggcccgatttttatgaccattccggcgtttttg
cgaaaaccagcgcggtgtataacccggtgatttatattatgatgaacaaacagtttcgcaccagcgcgcagcatgcgctgaccagcgtgagccg
cggcagcagcctgaaaattctgagcaaaggcaaacgcggcggccatagcagcgtgagcaccgaaagcgaaagcagcagctttcatagcagccgt
acgcaaccggtcgagatctgctgtacagtgagcaagggcgaggaggataacatggccatcatcaaggagttcatgcgcttcaaggtgcacatgg
agggctccgtgaacggccacgagttcgagatcgagggcgagggcgagggccgcccctacgagggcacccagaccgccaagctgaaggtgaccaa
gggtggcccccctgcccttcgcctgggacatcctgtccctcagttcatgtacggctccaaggcctacgtgaagcaccccgccgacatccccgac
tacttgaagctgtccttccccgagggcttcaagtgggagcgcgtgatgaacttcgaggacggcggcgtggtgaccgtgacccaggactcctccc
tccaggacggcgagttcatctacaaggtgaagctgcgcggcaccaacttccctccgacggccccgtaatgcagaagaagaccatgggctggga
ggcctcctccgagcggatgtaccccgaggacggcgccctgaagggcgagatcaagcagaggctgaagctgaaggacggcggccactacgacgct
gaggtcaagaccacctacaaggccaagaagcccgtgcagctgccggcgcctacaacgtcaacatcaagttggacatcacctcccacaacgagg
actacaccatcgtggaacagtacgaacgcgccgagggccgccactccaccggcggcatggacgagctgtacaagtag

Figure S2

Design of primers for inflSP_VSVG cloning. A silent mutation is inserted at GATATA sequence. The forward primer contains a starting sequence, specific restriction enzyme EcoRV (green), part of inflSP_VSVG (yellow) and sequence homologues to the base-construct DNA. The reverse primer contains a starting sequence, specific restriction enzyme EcoRV (green), second part of inflSP_VSVG (yellow) and sequence homologues to the base-construct DNA. Start codon and spot codon are colored red, the sequence of CXCR4 highlighted in blue, the sequence of mCherry - in pink.

4.6 Acknowlegement

We thank Harald Janovjak for valuable comments and discussion. Additionally we thank the Janovjak Lab for the opportunity to perform part of the cloning and analysis experiments at the IST in Vienna.

4.7 References

Airan, R.D., Thompson, K.R., Fenno, L.E., Bernstein, H., and Deisseroth, K. (2009). Temporally precise in vivo control of intracellular signalling. Nature 458, 1025-1029.

Arenkiel, B., Peca, J., Davison, I., Feliciano, C., Deisseroth, K., Augustine, G., Ehlers, M., and Feng, G. (2006). In Vivo Light-Induced Activation of Neural Circuitry in Transgenic Mice Expressing Channelrhodopsin-2. Neuron.

Bailes, H.J., Zhuang, L.-Y.Y., and Lucas, R.J. (2012). Reproducible and sustained regulation of Gas signalling using a metazoan opsin as an optogenetic tool. PLoS ONE 7, e30774.

Costanzi, S., Siegel, J., Tikhonova, I.G., and Jacobson, K.A. (2009). Rhodopsin and the others: a historical perspective on structural studies of G protein-coupled receptors. Curr. Pharm. Des. 15, 3994-4002.

Deretic, D. (1998). Post-Golgi trafficking of rhodopsin in retinal photoreceptors. Eye (Lond) 12 (Pt 3b), 526-530.

Deretic, D., Schmerl, S., Hargrave, P.A., Arendt, A., and McDowell, J.H. (1998). Regulation of sorting and post-Golgi trafficking of rhodopsin by its C-terminal sequence QVS(A)PA. Proc. Natl. Acad. Sci. U.S.A. 95, 10620-10625.

Fredriksson, R., Lagerstrom, M.C., Lundin, L.-G.G., and Schioth, H.B. (2003). The G-protein-coupled receptors in the human genome form five main families. Phylogenetic analysis, paralogon groups, and fingerprints. Mol. Pharmacol. 63, 1256-1272.

Hoffmann, C., Zurn, A., Bunemann, M., and Lohse, M.J. (2008). Conformational changes in G-protein-coupled receptors-the quest for functionally selective conformations is open. Br. J. Pharmacol. 153 Suppl 1, S358-66.

Hofmann, K., Scheerer, P., Hildebrand, P., Choe, H.-W., Park, J., Heck, M., and Ernst, O. (2009). A G protein-coupled receptor at work: the rhodopsin model. Trends in Biochemical Sciences.

Kim, J.-M.M., Hwa, J., Garriga, P., Reeves, P.J., RajBhandary, U.L., and Khorana, H.G. (2005). Light-driven activation of beta 2-adrenergic receptor signaling by a chimeric rhodopsin containing the beta 2-adrenergic receptor cytoplasmic loops. Biochemistry 44, 2284-2292.

Kochl, R., Alken, M., Rutz, C., Krause, G., Oksche, A., Rosenthal, W., and Schulein, R. (2002). The signal peptide of the G protein-coupled human endothelin B receptor is necessary for translocation of

the N-terminal tail across the endoplasmic reticulum membrane. J. Biol. Chem. 277, 16131-16138.

Liberman, J., Sartelet, H., Flahaut, M., Muhlethaler-Mottet, A., Coulon, A., Nyalendo, C., Vassal, G., Joseph, J.-M.M., and Gross, N. (2012). Involvement of the CXCR7/CXCR4/CXCL12 axis in the malignant progression of human neuroblastoma. PLoS ONE 7, e43665.

Mattis, J., Tye, K.M., Ferenczi, E.A., Ramakrishnan, C., O'Shea, D.J., Prakash, R., Gunaydin, L.A., Hyun, M., Fenno, L.E., Gradinaru, V., et al. (2012). Principles for applying optogenetic tools derived from direct comparative analysis of microbial opsins. Nat. Methods 9, 159-172.

Nagel, G., Szellas, T., Huhn, W., Kateriya, S., Adeishvili, N., Berthold, P., Ollig, D., Hegemann, P., and Bamberg, E. (2003). Channelrhodopsin-2, a directly light-gated cation-selective membrane channel. Proc. Natl. Acad. Sci. U.S.A. 100, 13940-13945.

Palczewski, K., Kumasaka, T., Hori, T., Behnke, C., Motoshima, H., Fox, B., Trong, I., Teller, D., Okada, T., Stenkamp, R., et al. (2000). Crystal Structure of Rhodopsin: A G Protein-Coupled Receptor. Science.

Rajagopalan, L., and Rajarathnam, K. (2006). Structural basis of chemokine receptor function–a model for binding affinity and ligand selectivity. Biosci. Rep. 26, 325-339.

Rein, M.L., and Deussing, J.M. (2012). The optogenetic (r)evolution. Mol. Genet. Genomics 287, 95-109.

Roche, S., Albertini, A.A., Lepault, J., Bressanelli, S., and Gaudin, Y. (2008). Structures of vesicular stomatitis virus glycoprotein: membrane fusion revisited. Cell. Mol. Life Sci. 65, 1716-1728.

Rosenkilde, M.M., Kledal, T.N., Holst, P.J., and Schwartz, T.W. (2000). Selective elimination of high constitutive activity or chemokine binding in the human herpesvirus 8 encoded seven transmembrane oncogene ORF74. J. Biol. Chem. 275, 26309-26315.

Saliba, R.S., Munro, P.M., Luthert, P.J., and Cheetham, M.E. (2002). The cellular fate of mutant rhodopsin: quality control, degradation and aggresome formation. J. Cell. Sci. 115, 2907-2918.

Sevier, C.S., Weisz, O.A., Davis, M., and Machamer, C.E. (2000). Efficient export of the vesicular stomatitis virus G protein from the endoplasmic reticulum requires a signal in the cytoplasmic tail that includes both tyrosine-based and di-acidic motifs. Mol. Biol. Cell 11, 13-22.

Tsukamoto, H., and Terakita, A. (2010). Diversity and functional properties of bistable pigments. Photochem. Photobiol. Sci.

Tye, K.M., and Deisseroth, K. (2012). Optogenetic investigation of neural circuits underlying brain disease in animal models. Nat. Rev. Neurosci. 13, 251-266.

Venkatakrishnan, A.J., Deupi, X., Lebon, G., Tate, C.G., Schertler, G.F., and Babu, M.M. (2013). Molecular signatures of G-protein-coupled receptors. Nature 494, 185-194.

Venkatesan (2003). Distinct Mechanisms of Agonist-induced Endocytosis for Human Chemokine Receptors CCR5 and CXCR4. Molecular Biology of the Cell.

Wess, J., Han, S.-J.J., Kim, S.-K.K., Jacobson, K.A., and Li, J.H. (2008). Conformational changes involved in G-protein-coupled-receptor activation. Trends Pharmacol. Sci. 29, 616-625.

Wu, B., Chien, E.Y., Mol, C.D., Fenalti, G., Liu, W., Katritch, V., Abagyan, R., Brooun, A., Wells, P., Bi, F.C., et al. (2010). Structures of the CXCR4 chemokine GPCR with small-molecule and cyclic peptide antagonists. Science 330, 1066-1071.

Xu, Y., Hyun, Y.-M.M., Lim, K., Lee, H., Cummings, R.J., Gerber, S.A., Bae, S., Cho, T.Y., Lord, E.M., and Kim, M. (2014). Optogenetic control of chemokine receptor signal and T-cell migration. Proc. Natl. Acad. Sci. U.S.A. 111, 6371-6376.